Fluorescence Time Delay in Multistep Auger Decay as an Internal Clock

S. Kosugi,[1,2] F. Koike,[1] M. Iizawa,[1,2,†] M. Oura,[2] T. Gejo,[2,3] K. Tamasaku,[2] J. R. Harries,[4] R. Guillemin,[5] M. N. Piancastelli,[2,5,6] M. Simon,[2,5] and Y. Azuma[1,2,*]

[1]*Department of Materials and Life Sciences, Sophia University, Tokyo 102-8554, Japan*
[2]*RIKEN SPring-8 Center, 1-1-1 Kouto, Sayo-cho, Sayo-gun, Hyogo 679-5148, Japan*
[3]*Graduate School of Materials Science, University of Hyogo, Kamigori-cho, Ako-gun 678-1297, Japan*
[4]*National Institutes for Quantum and Radiological Science and Technology, SPring-8, 1-1-1 Kouto, Sayo, Hyogo 679-5148, Japan*
[5]*Sorbonne Université, CNRS, UMR 7614, Laboratoire de Chimie Physique-Matière et Rayonnement, F-75005 Paris, France*
[6]*Department of Physics and Astronomy, Uppsala University, Box 516, SE-75120 Uppsala, Sweden*

(Received 13 November 2019; accepted 14 April 2020; published 8 May 2020)

Differences in postcollision interaction (PCI) effects on Kr $L_3M_{4,5}M_{4,5}$ Auger electron spectra were observed, depending on whether the initial photoionization occurred slightly above the K threshold or slightly above the L_3 threshold. For the former, KL fluorescence emission most likely happens and then Auger processes due to the L_3 hole follow. The time delay due to fluorescence causes a reduced shift of the Auger peak and tailing toward lower energy, since the Auger overtaking of the photoelectron happens later in time and at a location farther away from the ionic core, compared to the case for the simple one-step $L_3M_{4,5}M_{4,5}$ Auger decay after L-shell photoionization. Time-dependent theory for PCI in multistep processes agrees well with experiment, illustrating the effect as an internal clock for the time-sequence of the dynamical process.

DOI: 10.1103/PhysRevLett.124.183001

In atomic inner-shell photoionization processes near threshold, post-collision interaction (PCI) between the photoelectron and subsequently emitted Auger electrons occurs [1–12]. Generally, PCI is described as a sudden Coulomb potential change due to the fast Auger electrons overtaking a slow photoelectron. The photoelectron peak shifts and broadens towards lower kinetic energies, and the Auger electron peaks shift and broaden toward higher energies. For deep inner-shell photoionization near threshold, multiple electrons are released in the subsequent Auger cascade processes, and slow photoelectrons are overtaken by all the Auger electrons. All PCI effects in these cascading steps add up in the final photoelectron spectral deformation and shift.

Furthermore, for deep inner-shell ionizations, radiative transitions occur with considerable probability in the subsequent relaxation process [13–16]. Thus it is essential to investigate how fluorescence emission affects the PCI effect in multistep processes. Because there is no Coulombic interaction between photons and electrons, the radiative photoemission itself causes no PCI effects. However, the Auger process will be time delayed due to the core-hole lifetime in the cascading steps, which causes shift and change of the Auger line shape. In the classical picture, the overtaking happens at a later time, farther away from the ionic core. This time-delay effect has not been specifically examined before. In the cascade following the K-shell photoionization of Kr, there are mainly two decay pathways. One is a $2p \rightarrow 1s$ KL fluorescence emission process, and the other is KLL Auger decay. According to Kochur *et al.* [17], the branching ratio of the radiative and Auger decays following the $1s$ ionization of Kr is about 2∶1. Therefore, in the Auger spectroscopy near the K-shell ionization threshold (14327.2 eV [18]), it is important to consider the influence of fluorescence on PCI. Hayaishi *et al.* [1] measured ions in coincidence with zero-kinetic-energy electrons in the K shell photoionization of Kr with using threshold electron photoIon coincidence (TEPICO). A shift in the threshold electron peaks depending on coincident ion charge was noticed, and was attributed at least partially to the radiative decay participating in the cascade. However, there has been no direct observation of PCI profiles in the Auger electron spectrum significantly affected by the fluorescence emission except for some discussion without conclusive experimental result [2,3].

In this study, the Kr LMM Auger electron spectra were measured with photon energy tuned very close to the K-shell threshold. We concentrated on the $L_3M_{4,5}M_{4,5}$ Auger decay channel, although other Auger pathways are also open (KLL, KLM, $LL-LMM$, etc.) [15,16]. We observed the effect of PCI between the K-shell photoelectron and the LMM Auger electron emitted after KL fluorescence emission. For interpretation, we propose a time-dependent PCI theory for the multistep decay of a deep inner-shell vacancy state including the fluorescence effect. For comparison, we also measured the $L_3M_{4,5}M_{4,5}$ Auger electron spectrum following photoionization near the L_3 threshold (1678.4 eV [19]). We found significant differences in the

shift and spectral profiles between the K-shell threshold and the L_3-shell threshold. Our theory reproduces the differences reasonably well.

Experiments were performed at the x-ray beam lines BL19LXU [20] and BL17SU [21,22] at SPring-8 in Japan. At BL19LXU, linearly polarized light was delivered from an in-vacuum 27-m long 780 periods undulator [23]. The photon energy was set to 14.2–14.4 keV (near the K threshold) by the Si (111) double-crystal monochromator [24]. The photon band pass was calculated to be 2.0 eV at 14.4 keV and the photon flux was of the order of 10^{14} photons/s. At BL17SU, photon energies between 300 and 2000 eV were available. The typical resolving power $E/\Delta E$ of the monochromator was greater than 10000 and photon flux was of the order of 10^{11} photons/s. The photon beams were passed through a gas-cell (Scienta GC-50). Electrons were measured by a hemispherical electron energy analyzer (Scienta SES-2002) [15], with energy resolution set to 0.4 eV. The photon energy scale was calibrated by fitting a total ion yield spectrum to the photoionization cross section curve of Schaphorst *et al.* [18] (Kr $1s$) and Hubbell *et al.* [25] (Kr $2p$). The energy scale of the analyzer was corrected by measuring the $L_3M_{4,5}M_{4,5}$ ($^1G_4$) nominal (without PCI shift) Auger line [26].

Our theoretical calculation is based on a time-dependent framework. Koike [4] pointed out that electronic wave functions are continuous and smooth with respect to any sudden change of potential, and consequently the local wave numbers of both electrons are conserved for points equidistant from the atomic center. Physically, this corresponds to the postulate that the local electronic momenta do not change at the instance of overtaking. Applying the continuity of log derivatives to the two electronic radial wave functions, we can derive the following spectral profile function $P(\varepsilon)$ of the photoelectron energy ε.

$$P(\varepsilon) = \left| \int_0^\infty dt_i \exp\left(-i \int_0^{t_i} \left(\varepsilon - \frac{i}{2}\Gamma_i + \frac{1}{\overline{r_i}} \right) dt \right) \right|^2, \quad (1)$$

where, t_i is the instance of Auger electron emission measured from the instance of photoelectron emission, Γ_i is the Auger width, and $\overline{r_i}$ is the radial distance from the atomic center where the two electrons influence each other. For a given time t, $\overline{r_i}$ is the solution to

$$\int_0^{\overline{r_i}} \left(\frac{1}{v_1} - \frac{1}{v_i} \right) dr = t, \quad (2)$$

with the local velocities v_1 and v_i for the photoelectron and the Auger electron, respectively. Atomic units ($e = \hbar = m = 1$) are used here. For multiple electron escape such as Auger cascade after a deep inner-shell photoionization, we can straightforwardly extend Eq. (1) if the photoelectron is overtaken by all Auger electrons [5]. For the case of n-electron escape,

$$P(\varepsilon) = \left| \begin{array}{c} \int_0^\infty dt_n \int_0^{t_n} dt_{n-1} \ldots \int_0^{t_3} dt_2 \\ \times \exp\left(-i \int_0^{t_n} \left(\varepsilon - i\frac{\gamma(t)}{2} + \delta(t) \right) dt \right) \end{array} \right|^2, \quad (3)$$

with a width function $\gamma(t) = \sum_{i=q}^{n} \Gamma_i$ and a shift function $\delta(t) = \sum_{i=2}^{q} 1/\overline{r_i}$ for $t_{q-1} < t < t_q$ with $q = 2, 3, \ldots n$. The profile formula given in Eq. (3) has been applied to the cascading Auger decay after the Ar K-shell photoionization [6] and the theory has well reproduced the TEPICO spectra by Hayaishi *et al.* [7].

We can apply Eq. (3) with minor modifications to the present case of L-shell Auger electron emission preceded by K-shell radiative photon emission decay. Because there is no Coulomb interaction between a photon and an electron, we should replace $1/\overline{r_i}$ by 0 for photon emissions, i.e., we replace $1/\overline{r_2}$ by 0 in the present case. The shift function becomes $\delta(t) = 0$ for $t_1 = 0 < t < t_2$ and $\delta(t) = 1/\overline{r_3}$ for $t_2 < t < t_3$. The width function becomes $\gamma(t) = \Gamma_2 + \Gamma_3$ for $t_1 = 0 < t < t_2$ and $\gamma(t) = \Gamma_3$ for $t_2 < t < t_3$. Thus the spectral profile will have no PCI shift but only the effect of lifetime broadening by radiative decay. The present formula also takes into account the delay of Auger electron emission waiting for the preceding radiative decay. Further, we can regard Eq. (3) as the energy gain spectrum of Auger electron by simply reversing the sign of $\delta(t)$ in the equation due to energy conservation of the system; the emitted K-shell radiative photons have no electric charge and no effect on the energy exchange among the emitted particles.

Figure 1 shows our measured Kr $L_3M_{4,5}M_{4,5}$ Auger electron spectra at excess energies (incident photon energy —Kr $1s$ ionization threshold energy) $=E_{\rm exc} = 0.6$, 5.6, and 95.6 eV with the spectra obtained with Eq. (3). The results at $E_{\rm exc} = -54.4$ eV are also given in the inset, which are attributed to normal Auger spectra following direct photoionization of the L_3 shell.

Because the K-shell ionization channel is open for $E_{\rm exc} > 0$, the Kr $L_3M_{4,5}M_{4,5}$ spectral profiles for positive $E_{\rm exc}$ are considered as mainly from L_3 vacancy produced by K_α fluorescence following K-shell photoionization. Asymmetric and broadened line shapes due to the PCI effect are confirmed in these spectral profiles. The $L_3M_{4,5}M_{4,5}$ ($^1G_4$) Auger peak shifts from the nominal energy position as a function of the decrease of excess energy $E_{\rm exc}$, which agrees with the general behavior of PCI. However, we observe that the spectral tail on the lower energy wing is enhanced considerably, which is not expected in the usual one-step PCI.

The result of theoretical calculations using Eq. (3) is also given in Fig. 1 by solid (crimson) curves, which agrees well with experiment. The theory takes into account the radiative decay of the K shell preceding the Auger decay of the L_3 shell. For the numerical calculation, the K-shell lifetime

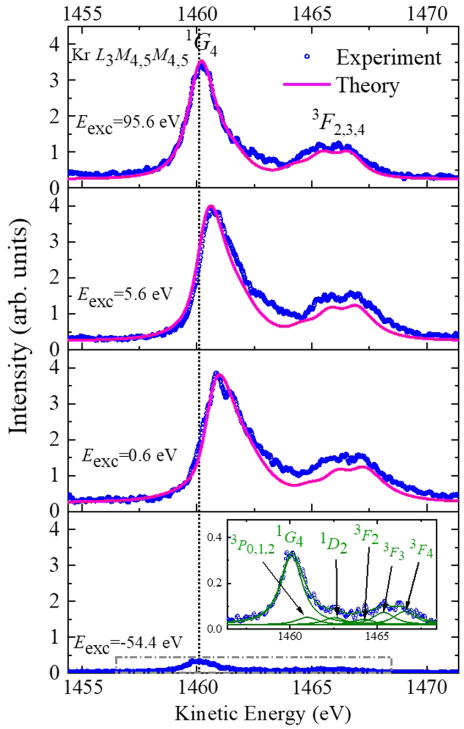

FIG. 1. Kr $L_3M_{4,5}M_{4,5}$ Auger electron spectra near the K threshold for several excess energies E_{exc}. Assignments are from $2p$ photoionization studies [26]. The vertical dotted line at 1460.1 eV shows the nominal $L_3M_{4,5}M_{4,5}$ ($^1G_4$) Auger energy [26]. The solid curves are superpositions of Eq. (3) for two-step cascades with $\Gamma_{2p} = 1.17$ and $\Gamma_{1s} = 3.92$ eV [27], and spectral heights normalized to experiment at the $^1G_4$ peaks.

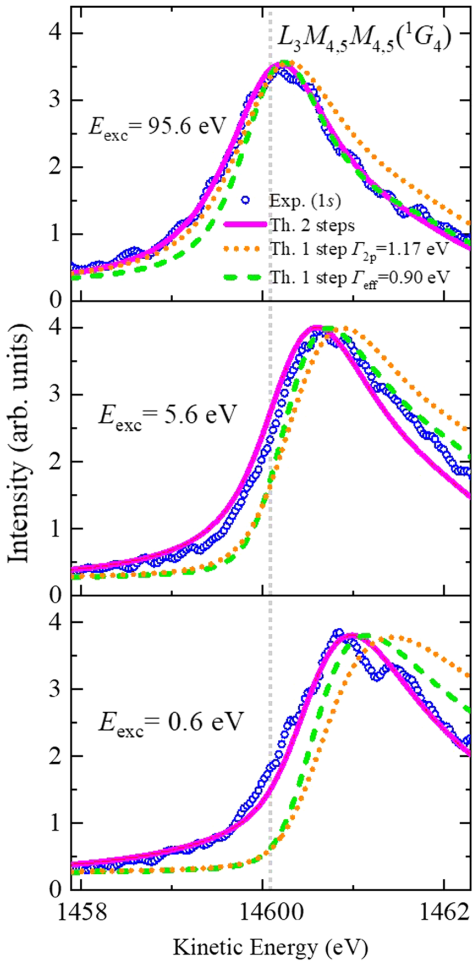

FIG. 2. The Kr $L_3M_{4,5}M_{4,5}$ ($^1G_4$) Auger line for $E_{exc(1s)} = 95.6$, 5.6, and 0.6 eV. Open (blue) circles: present experiment. Solid (crimson) curves: two-step decay model [Eq. (3)] with $\Gamma_{2p} = 1.17$ and $\Gamma_{1s} = 3.92$ eV [27]. Dotted (orange) curve: one-step decay model with $\Gamma_{2p} = 1.17$ eV. Broken (light green) curve: one-step effective decay width model with $\Gamma_{eff} = 0.90$ eV. Theoretical curves are convoluted with $\Gamma_{3d}^2 = 0.16$ eV [28] and the experimental resolution. The vertical dotted line at 1460.1 eV shows the nominal $L_3M_{4,5}M_{4,5}$ ($^1G_4$) Auger energy [26].

width of $\Gamma_{1s} = 3.92$ eV [27] and the L-shell lifetime width of $\Gamma_{2p} = 1.17$ eV [27] were adopted.

To adjust the calculated spectra to experimental conditions, theoretical curves were convoluted with a Lorentzian of 0.16 eV FWHM that simulates the spread of the Kr^{2+} ($3d^{-2}$) state energy (which is twice the 0.08 eV [28] of the $3d^{-1}$ single core states) and with a Gaussian that simulates the total experimental resolution [8]. The effects in the experimental spectrum from any contribution from the LMM Auger process due to L-shell photoionization way above the threshold are negligible. The intensity ratio should be considerably less than one-tenth according to the cross sections and fluorescence branching ratio quoted in Kochur [17], so L-shell ionization was not included in the theoretical calculation.

Figure 2 illustrates several PCI profiles of the Kr $L_3M_{4,5}M_{4,5}$ ($^1G_4$) Auger line, to compare the present results with effective lifetime model interpretations. In previous papers [2,3], PCI effects including radiative decay were explained in a one-step framework PCI model using an effective lifetime width $\Gamma_{eff} = \Gamma_{2p}\Gamma_{1s}/(\Gamma_{2p} + \Gamma_{1s})$. When the K-shell fluorescence emission of lifetime $\tau_{1s} = \hbar/\Gamma_{1s}$ precedes the L-shell Auger decay of lifetime $\tau_{2p} = \hbar/\Gamma_{2p}$, the effective lifetime of L-shell Auger electron emission after the K-shell photoionization τ_{eff} may be assumed to be the sum of τ_{1s} and τ_{2p}, i.e., $\tau_{eff} = \tau_{1s} + \tau_{2p}$ as a working hypothesis. Figure 2 shows the experimental PCI profiles of the Kr $L_3M_{4,5}M_{4,5}$ ($^1G_4$) Auger line for excess energies $E_{exc(1s)} = 95.6$, 5.6, and 0.6 eV, together with the theoretical profiles of the present two-step model [Eq. (3)] with $\Gamma_{2p} = 1.17$ and $\Gamma_{1s} = 3.92$ eV [27], the effective lifetime width model with $\Gamma_{eff} = \Gamma_{2p}\Gamma_{1s}/(\Gamma_{2p} + \Gamma_{1s}) = 0.90$ eV, and the simple one-step model with $\Gamma_{2p} = 1.17$ eV. The effective lifetime width model does not satisfactorily reproduce the experimental PCI profiles. The deviation from the experiment is particularly large for the lowest excess energies. It is clear

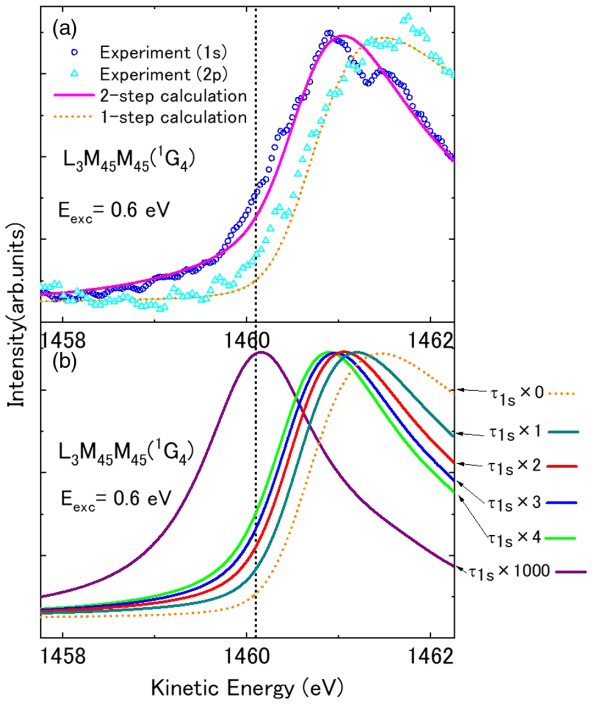

FIG. 3. (a) The Kr $L_3M_{4,5}M_{4,5}$ ($^1G_4$) Auger line for $E_{\mathrm{exc}} = 0.6$ eV. Open circles (blue): experiment above the $1s$ threshold. Open triangles (light blue): experiment above the $2p$ threshold. Solid curve (crimson): theory for two-step decay [Eq. (3)] with $\Gamma_{2p} = 1.17$, $\Gamma_{1s} = 3.92$ eV [27]. Dotted curve (orange): theory for one-step decay [Eq. (1)] with $\Gamma_{2p} = 1.17$ eV. (b) Simplified fluorescence time delay model [Eq. (4)], for delay times $T = \tau_{1s} \times 0$, 1, 2, 3, 4, 1000, where $\tau_{1s} = 168$ as is the K-shell lifetime. $T = \tau_{1s} \times 0$ corresponds to no fluorescence time delay, and $T = \tau_{1s} \times 1000$ to no PCI.

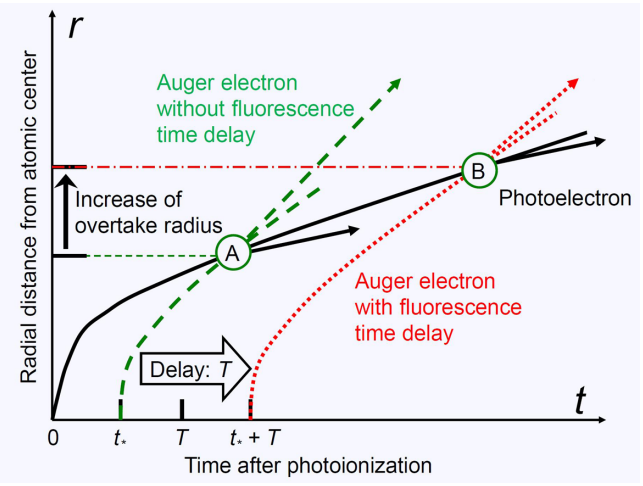

FIG. 4. Schematic of the fluorescence time delay effect on the PCI. The solid (black) curve shows the photoelectron radial distance r against time t. The broken (green) and dotted (red) curves are for Auger electrons without and with fluorescence delay time T, respectively. The Auger electrons overtake the photoelectron at points A and B. The r at B is larger than at A, so the PCI effect is weaker.

that the effect of having no Auger electrons before the fluorescence emission has to be incorporated in the theory.

The present measurement of the Kr $L_3M_{4,5}M_{4,5}$ Auger spectra near the L_3 threshold further clarifies the influence of the KL fluorescence emission in the PCI spectral profiles near the K-shell threshold. A direct comparison between Auger spectra measured close either to the K-shell or to the L-shell threshold is shown in Fig. 3(a). The PCI spectral profiles of the Kr $L_3M_{4,5}M_{4,5}$ ($^1G_4$) Auger line for excess energy $E_{\mathrm{exc}(2p)} = 0.6$ eV is compared with our one-step Eq. (1) calculation using the lifetime width $\Gamma_{2p} = 1.17$ eV [27]. Theory and experiment agree well, both with energy shift and spread of the peak. Figure 3(a) also shows the spectrum of $L_3M_{4,5}M_{4,5}$ ($^1G_4$) Auger line for excess energy $E_{\mathrm{exc}(1s)} = 0.6$ eV, which shows that there is a difference between $E_{\mathrm{exc}(1s)} = 0.6$ and $E_{\mathrm{exc}(2p)} = 0.6$ eV, in both peaks broadening and energy shift. It is confirmed that the lower energy tail not seen in the PCI structure of one-step Auger decay, appears in the two-step spectra close to K threshold.

To make the physical significance of the present effect clear, we try to directly consider the fluorescence time delay in the profile formation of the Auger electron spectrum. We take T as the time of the K-hole decay after the instant of K-shell photoionization, which is typically the lifetime of the K-shell vacancy states $\tau_{1s} = 168$ as. This value was derived from the K-hole width quoted in Ref. [27]. Because the Auger decay takes place after the fluorescence emission at time T, we replace the starting point of the time integration 0 with T in Eq. (1), giving

$$P(\varepsilon) = \left| \int_T^{\infty} dt_i \exp\left(-i \int_T^{t_i} \left(\varepsilon - \frac{i}{2}\Gamma_i + \frac{1}{\overline{r_i}} \right) dt \right) \right|^2 \qquad (4)$$

for the profile formula within the framework of a one-step Auger transition after the fluorescence decay. In Fig. 4, we give a schematic illustration showing the decrease of energy exchange between the photoelectron and the LMM Auger electron due to the delay of the Auger decay waiting for the K-shell fluorescence decay. Because the photoelectron can travel out of the atomic system before time T, the overtaking radius $\overline{r_i}$ for Auger electron becomes larger compared to the case without the fluorescence emission, causing a reduction of the energy exchange in the PCI. Thus, the effect of PCI will be decreased depending on the magnitude of T. In Fig. 3(b), we illustrate the calculated spectral profiles for $T = 0$, 1, 2, 3, 4, and 1000 times the Kr K-hole lifetime $\tau_{1s} = 168$ as. The spectrum shifts to lower energies with increased T. The spectrum also changes shape, converging to a Lorentzian with L-shell lifetime width $\Gamma_{2p} = 1.17$ eV at $T \to \infty$. Comparing these results with the experimental curves in Fig. 3(a), we find that theory fits best to experiment at around $T = T_d = 2\tau_{1s} = 336$ as. The optimum delay time T_d agrees fairly

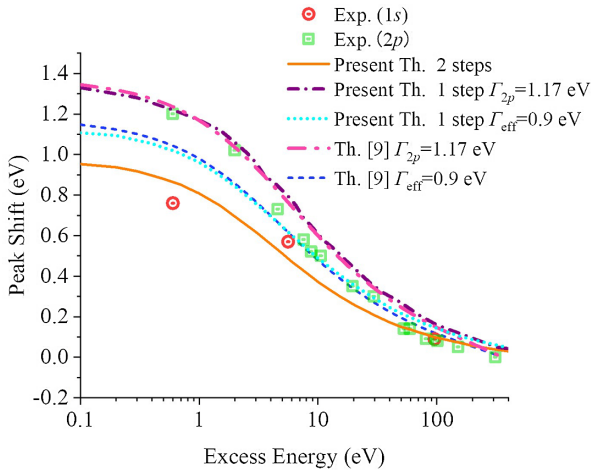

FIG. 5. The PCI shifts of Kr $L_3M_{4,5}M_{4,5}$ $^1G_4$ Auger line. Open (red) circles: K-shell photoionization. Open (green) squares: L-shell photoionization. Solid (orange) curve: two-step model [Eq. (3)]. Dot-dashed (purple) curve: one-step model with $\Gamma_{2p} = 1.17$ eV [Eq. (1)]. Dotted (light blue) curve: one-step model with $\Gamma_{\rm eff} = 0.90$ eV. Dot-dashed (crimson) curve: semiclassical model [9] for $\Gamma_{2p} = 1.17$ eV. Broken (blue) curve: same for $\Gamma_{\rm eff} = 0.90$ eV.

well with the K-shell vacancy lifetime τ_{1s}. Because in an actual system the time T will obey the Poisson probability distribution $(\hbar/\tau_{1s})\exp(-\hbar T/\tau_{1s})$, it is natural that T_d differs slightly from τ_{1s}. We can apply a more sophisticated version of the profile formula given in Eq. (3) to obtain a better delay time. We can also verify that $\Gamma_{1s} = 3.92$ eV ($\tau_{1s} = 168$ as) results in the best fit to the experiments as found in Fig. 3(a). We can therefore point out that the difference of PCI effects between the cases of K-shell and L-shell photoionization works as an internal clock to directly measure the fluorescence lifetime in the time domain.

Figure 5 shows the PCI peak shifts of $L_3M_{4,5}M_{4,5}$ Auger lines for the $^1G_4$ state as a function of excess energy $E_{\rm exc}$. The theory and experiment agree well in both cases that start from K-shell and L-shell photoionizations. The simulated one-step model calculation using the effective width $\Gamma_{\rm eff} = \Gamma_{2p}\Gamma_{1s}/(\Gamma_{2p} + \Gamma_{1s}) = 0.90$ eV differs from experiment at lower excess energies. Semiclassical calculations using a formula by van der Straten *et al.* [9] are also given for comparison.

A measurement of the PCI shift by direct L-shell ionization was also done by Suzuki *et al.* [10]. However, the experimental values of their energy shifts are considerably lower than our experimental values. The probable reason for this difference is that they assumed the $L_3M_{4,5}M_{4,5}$ ($^1G_4$) Auger line at 1725 eV to be the nominal Auger line, whereas an appreciable PCI shift actually remained at this photon energy.

In a pioneering work [29] it was shown that the PCI shift can be used as "streaking" to measure the lifetime of the interatomic Coulombic decay (ICD) process in He dimers. However, the full potential of PCI to derive quantitative information not only in the energetics domain, but even in the time domain, has not yet been exploited.

In conclusion, we have reported the observation of PCI effects in the Kr $L_3M_{4,5}M_{4,5}$ line with photon energy slightly above the K threshold. The energy shift and broadening were observed in the LMM Auger spectra following KL fluorescence emission. Decreased energy shift and tailing to the lower energy side, which is not seen in the PCI structure of ordinary one-step Auger decay, appeared within the spectra close to threshold. We proposed a time-dependent theory of PCI multistep processes from which we obtained a good agreement with experimental results. In addition, we showed experimentally and theoretically that the PCI profile of Kr $L_3M_{4,5}M_{4,5}$ Auger spectra observed near the L_3 threshold without any fluorescence effect is different in both the broadening and the energy shift compared to the spectrum near the K threshold. Our results demonstrate that the PCI process effectively acts as an internal clock with 100 as timescale, which can be used to measure sequential timing within multistep decay dynamics.

The experiment was conducted at BL19LXU and BL17SU beamlines of SPring-8 under the approval of RIKEN proposal No. 20170028. Y. A., S. K., and M. I. thank the JSPS Gant-in Aid Category C. The authors are grateful to the technical staff of BL19LXU and BL17SU for assistance.

*Corresponding author.
y-azuma@sophia.ac.jp
†Present address: Department of Physics, Rikkyo University, Tokyo 171-8501, Japan.

[1] T. Hayaishi, Y. Fujita, M. Izumisawa, T. Tanaka, E. Murakami, E. Shigemasa, A. Yagishita, and Y. Morioka, J. Phys. B **33**, 37 (2000).
[2] R. Guillemin, S. Sheinerman, C. Bomme, L. Journel, T. Marin, T. Marchenko, R. K. Kushawaha, N. Trcera, M. N. Piancastelli, and M. Simon, Phys. Rev. Lett. **109**, 013001 (2012).
[3] U. Arp, T. LeBrun, S. H. Southworth, M. A. MacDonald, and M. Jung, Phys. Rev. A **55**, 4273 (1997).
[4] F. Koike, J. Phys. Soc. Jpn. **57**, 2705 (1988).
[5] F. Koike, Phys. Lett. A **193**, 173 (1994).
[6] F. Koike, Nucl. Instrum. Methods Phys. Res., Sect. B **267**, 231 (2009).
[7] T. Hayaishi, E. Murakami, Y. Morioka, E. Shigemasa, A. Yagishita, and F. Koike, J. Phys. B **27**, L115 (1994).
[8] R. Guillemin, S. Sheinerman, R. Püttner, T. Marchenko, G. Goldsztejn, L. Journel, R. K. Kushawaha, D. Céolin, M. N. Piancastelli, and M. Simon, Phys. Rev. A **92**, 012503 (2015).
[9] P. van der Straten, R. Morgenstern, and A. Niehaus, Z. Phys. D **8**, 35 (1988).

[10] I. H. Suzuki, A. Fujii, S. Nagaoka, M. Kosugi, K. Okada, T. Ibuki, S. Samori, Y. Tamenori, and H. Ohashi, J. Phys. B **37**, 1433 (2004).
[11] S. Kosugi, M. Iizawa, Y. Kawarai, Y. Kuriyama, A. L. D. Kilcoyne, F. Koike, N. Kuze, D. S. Slaughter, and Y. Azuma, J. Phys. B **48**, 115003 (2015).
[12] S. Kosugi, N. Suzuki, N. Kumagai, H. Iwayama, E. Shigemasa, F. Koike, and Y. Azuma, J. Phys. B **52**, 245002 (2019).
[13] M. N. Piancastelli, K. Jänkälä, L. Journel, T. Gejo, Y. Kohmura, M. Huttula, M. Simon, and M. Oura, Phys. Rev. A **95**, 061402(R) (2017).
[14] N. Boudjemia, K. Jänkälä, T. Gejo, K. Nagaya, K. Tamasaku, M. Huttula, M. N. Piancastelli, M. Simon, and M. Oura, Phys. Chem. Chem. Phys. **21**, 5448 (2019).
[15] M. Oura, T. Gejo, K. Nagaya, Y. Kohmura, K. Tamasaku, L. Journel, M. N. Piancastelli, and M. Simon, New J. Phys. **21**, 043015 (2019).
[16] N. Boudojemia *et al.*, Phys. Rev. A **101**, 053405 (2020).
[17] A. G. Kochur, V. L. Sukhorukov, A. I. Dudenko, and Ph. V. Demekhin, J. Phys. B **28**, 387 (1995).
[18] S. J. Schaphorst, A. F. Kodre, J. Ruscheinski, B. Crasemann, T. Åberg, J. Tulkki, M. H. Chen, Y. Azuma, and G. S. Brown, Phys. Rev. A **47**, 1953 (1993).
[19] S. Nagaoka, T. Ibuki, N. Saito, Y. Shimizu, Y. Senba, K. Kamimori, Y. Tamenori, H. Ohashi, and I. H. Suzuki, J. Phys. **B33**, L605 (2000).
[20] M. Yabashi, T. Mochizuki, H. Yamazaki, S. Goto, H. Ohashi, K. Takeshita, T. Ohata, T. Matsushita, K. Tamasaku, Y. Tanaka, and T. Ishikawa, Nucl. Instrum. Methods Phys. Res., Sect. A **467–468**, 678 (2001).
[21] H. Ohashi *et al.*, AIP Conf. Proc. **879**, 523 (2007).
[22] Y. Senba, H. Ohashi, H. Kishimoto, T. Miura, S. Goto, S. Shin, T. Shintake, and T. Ishikawa, AIP Conf. Proc. **879**, 718 (2007).
[23] T. Hara, M. Yabashi, T. Tanaka, T. Bizen, S. Goto, M. Marechal, T. Seike, K. Tamasaku, T. Ishikawa, and H. Kitamura, Rev. Sci. Instrum. **73**, 1125 (2002).
[24] T. Mochizuki, Y. Kohmura, A. Awaji, Y. Suzuki, A. Baron, K. Tamasaku, M. Yabashi, H. Yamazaki, and T. Ishikawa, Nucl. Instrum. Methods Phys. Res., Sect. A **467–468**, 647 (2001).
[25] J. H. Hubbell, P. N. Trehan, N. Singh, B. Chand, D. Mehta, M. L. Garg, R. R. Garg, S. Singh, and S. Puri, J. Phys. Chem. Ref. Data **23**, 339 (1994).
[26] J. C. Levin, S. L. Sorensen, B. Crasemann, M. H. Chen, and G. S. Brown, Phys. Rev. A **33**, 968 (1986).
[27] M. O. Krause, J. Phys. Chem. Ref. Data **8**, 307 (1979).
[28] E. Kukk, H. Aksela, A. Kivimäki, J. Jauhiainen, E. Nõmmiste, and S. Aksela, Phys. Rev. A **56**, 1481 (1997).
[29] F. Trinter, J. B. Williams, M. Weller, M. Waitz, M. Pitzer, J. Voigtsberger, C. Schober, G. Kastirke, C. Müller, C. Goihl, P. Burzynski, F. Wiegandt, T. Bauer, R. Wallauer, H. Sann, A. Kalinin, L. Ph. H. Schmidt, M. Schöffler, N. Sisourat, and T. Jahnke, Phys. Rev. Lett. **111**, 093401 (2013).